J Appl Physiol
89: 1699–1708, 2000.

Sequential $\dot{V}_A/\dot{Q}$ distributions in the normal rabbit by micropore membrane inlet mass spectrometry

JAMES E. BAUMGARDNER, IN-CHEOL CHOI, ANTON VONK-NOORDEGRAAF, H. FREDERICK FRASCH, GORDON R. NEUFELD, AND BRYAN E. MARSHALL
Department of Anesthesia, University of Pennsylvania, Philadelphia, Pennsylvania 19104-4283

Received 26 April 1999; accepted in final form 30 May 2000

Baumgardner, James E., In-Cheol Choi, Anton Vonk-Noordegraaf, H. Frederick Frasch, Gordon R. Neufeld, and Bryan E. Marshall. Sequential $\dot{V}_A/\dot{Q}$ distributions in the normal rabbit by micropore membrane inlet mass spectrometry. *J Appl Physiol* 89: 1699–1708, 2000.—We developed micropore membrane inlet mass spectrometer (MMIMS) probes to rapidly measure inert-gas partial pressures in small blood samples. The mass spectrometer output was linearly related to inert-gas partial pressure (r^2 of 0.996–1.000) and was nearly independent of large variations in inert-gas solubility in liquid samples. We infused six inert gases into five pentobarbital-anesthetized New Zealand rabbits and used the MMIMS system to measure inert-gas partial pressures in systemic and pulmonary arterial blood and in mixed expired gas samples. The retention and excretion data were transformed into distributions of ventilation-to-perfusion ratios ($\dot{V}_A/\dot{Q}$) with the use of linear regression techniques. Distributions of $\dot{V}_A/\dot{Q}$ were unimodal and broad, consistent with prior reports in the normal rabbit. Total blood sample volume for each $\dot{V}_A/\dot{Q}$ distribution was 4 ml, and analysis time was 8 min. MMIMS provides a convenient method to perform the multiple inert-gas elimination technique rapidly and with small blood sample volumes.

inert gases; multiple inert-gas elimination technique; solubility; stirring effect

THE DEVELOPMENT OF THE MULTIPLE inert-gas elimination technique (MIGET) by Wagner and coworkers in 1974 was a major advance in the study of pulmonary gas exchange (15, 36, 39). In MIGET, data on the retention [systemic arterial inert-gas partial pressure divided by mixed venous inert-gas partial pressure ($P\bar{v}$)] and excretion (mixed expired inert-gas partial pressure divided by $P\bar{v}$) of six infused inert gases are transformed into a distribution of ventilation-to-perfusion ratios ($\dot{V}_A/\dot{Q}$) in the lung (36, 38, 40). MIGET has been used to study the mechanisms of impaired gas exchange in several diseases and animal models of disease, including pneumonia (11, 35), asthma (19, 29), chronic obstructive pulmonary disease (2, 7, 26), atelectasis (33, 34), and acute respiratory distress syndrome (6, 44).

Despite its utility in providing unique information about the mechanisms of pulmonary gas exchange, MIGET has been applied by only a few research laboratories around the world (2, 7, 10, 11, 17, 26–28, 30, 33, 36, 43). In traditional MIGET, the inert-gas partial pressures in the blood samples are measured by gas chromatography (GC), which requires a time-consuming extraction of the inert gas into a gas phase before the GC analysis. The substantial analysis time (~3 h for each measurement of the 6 retention and excretion ratios) and the technical complexity of measuring inert-gas partial pressures in blood samples by GC have limited the use of MIGET in research applications and in the real-time clinical care of critically ill patients. For highest accuracy and reproducibility of the inert-gas extraction, traditional MIGET by GC also requires ~20 ml of blood sample for a single $\dot{V}_A/\dot{Q}$ determination, which has limited the applications of MIGET in pediatric medicine and in research studies in small animal models.

Membrane inlet mass spectrometry (MIMS) offers an alternative method for the analysis of inert-gas partial pressures in blood samples. In MIMS, a polymer membrane separates an aqueous sample from the vacuum chamber of the mass spectrometer, and volatile substances dissolved in the aqueous sample diffuse across the membrane into the vacuum system for mass spectrometer analysis (3, 18, 41). Prior investigators have applied MIMS to the measurement of inert-gas partial pressures in blood samples for six gases suitable for MIGET, with promising results (23, 24). A major limitation of MIMS, however, has been a dependence of the mass spectrometer signal on the inert-gas solubility in blood samples (23). Dependence of the signal on solubility can be reduced by the use of very thick membranes for MIMS, but thick membranes result in prohibitively slow response times (42). As a result, no practical ways of utilizing MIMS for MIGET have been reported.

Micropore membrane inlet mass spectrometry (MMIMS) provides a unique combination of rapid response speed and minimal dependence of the signal on inert-gas solubility in the aqueous sample (1). In MMIMS, the membrane is confined to a small pore. The membrane is thin, resulting in a fast response

Address for reprint requests and other correspondence: J. E. Baumgardner, Dept. of Anesthesia, Univ. of Pennsylvania, 3400 Spruce St., Philadelphia, PA 19104-4283 (E-mail: jbaumgar@mail.med.upenn.edu).

The costs of publication of this article were defrayed in part by the payment of page charges. The article must therefore be hereby marked "*advertisement*" in accordance with 18 U.S.C. Section 1734 solely to indicate this fact.

time, but the dependence of the signal on solubility is minimized by the three-dimensional diffusion profiles around the pore (1). MMIMS can, therefore, rapidly and directly measure the partial pressures of inert gases dissolved in aqueous samples, eliminating the extraction of inert gases into a gas phase that is required for GC analysis.

We developed MMIMS probes specifically designed for the measurement of trace concentrations of inert gases in small blood samples, and we applied this MMIMS technique to determine $\dot{V}_A/\dot{Q}$ distributions in normal rabbits by MIGET.

METHODS

MMIMS. Pores sealed with a polymer membrane were created in the ends of stainless steel tubing, as previously described (1). Briefly, 304 stainless steel tubing (1/16 in. OD, 0.040 in. ID), which was sealed on one end with a hemispherical cap weld of constant wall thickness throughout the weld (MicroGroup, Medway, MA), was mounted on a vacuum system. The sealed end of the tubing was filed at an angle of ~30° to the axis of the tubing while the helium leak rate into the vacuum system was monitored, until a leak was created large enough to register a helium current in the range of $1.5–14 \times 10^{-10}$ A on a quadrupole mass spectrometer (UTI 100C, see below for details, in Faraday cup mode). Although the size of the pores for this MMIMS probe was not directly assessed, the pore diameters for similar probes with larger helium leak rates have been estimated at 28 μm (1). After an appropriate helium leak rate was achieved, the pore (or pores, see Ref. 1) in the flat, filed surface at the tip of the probe was sealed with silicone adhesive sealant (Permatex 66B, Loctite, Cleveland, OH). Silicone was used in this probe, instead of the polytetrafluoroethylene vacuum grease used in prior MMIMS probes (1), to enhance sensitivity, because silicone polymers can be several hundred times more permeable to the inert gases of interest than polytetrafluoroethylene-based polymers (21). After the silicone had cured for 24 h, the probe was rotated 90°, and the shaving process was repeated. The probe was then rotated another 90°, and the process was repeated once more. The resulting probe had three flat, filed, pore-containing areas at its tip and, therefore, approximately three times as much sensitivity as a probe with a single filed area.

As in prior MMIMS systems (1), the stainless steel tubing was mounted on the vacuum system on a bored-through high-vacuum fitting, so that the tubing extended into the vacuum system and the tube opening was positioned adjacent to the ion source filaments. The total length of tubing between the probe tip and the ion source was 220 mm. The ion source and proximal part of the probe tubing were heated with heating tapes and insulation, with the source kept at 125°C.

The quadrupole mass spectrometer (model 100C, Uthe Technology International, Sunnyvale, CA) had an open grid, long path length electron impact ion source operating at 70 eV, a quadrupole filter with an aperture of 10.0 mm diameter, and a copper-beryllium electron multiplier with the voltage set at 1,714 V [gain at 28 atomic mass units (amu) of 4.8×10^4]. The all-metal vacuum system was wrapped in heating tapes and high-temperature insulation and was extensively baked after atmospheric exposures. Base pressure was $<1 \times 10^{-10}$ Torr. The vacuum system was evacuated by a turbomolecular pump (Turbovac 150, Leybold-Heraus, Export, PA) backed by a rotary vane pump (D8A, Leybold-Heraus), and the turbomolecular pump was connected to the vacuum chamber by a right-angle, high-vacuum isolation valve (model 951–5027, Varian, Lexington, MA). The valve was completely opened during bakeout and between experiments but was nearly closed during experiments to decrease the pumping speed and increase sensitivity. Vacuum system pressure during experiments was 7×10^{-8} Torr.

Inert-gas partial pressures in gas and liquid samples. The six inert gases were chosen to span evenly a large range of solubility in blood and to minimize spectral overlap during the mass spectrometer analysis. The six inert gases were sulfur hexafluoride (SF_6; Air Products and Chemicals, Allentown, PA), krypton (Kr; BOC Group, Murray Hill, NJ), desflurane (DES; Ohmeda, Liberty Corner, NJ), enflurane (ENF; Ohmeda), diethyl ether (DEE; Fisher Scientific, Fair Lawn, NJ), and acetone (ACT; EM Science, Cherry Hill, NJ). These inert gases are nearly identical to the series used by Mastenbrook et al. (24), but with DES substituted for freon-12. All inert gases were measured by using single-ion monitoring, with the peak location and switching controlled by a computer and interface (Spectralink, UTI, Sunnyvale, CA) and custom software (QDot, Kirtland, NM). The amu peaks selected for monitoring each gas were SF_6 at 127, Kr at 84, DES at 101, ENF at 117, DEE at 59, and ACT at 58 amu.

The time response of the system for each gas was assessed with step changes in inert-gas partial pressures for each gas individually, in both the gas phase and liquid phase. Absence of vacuum system memory effects was confirmed by following the signal after a step decrease in inert-gas partial pressure.

Sensitivity of the mass spectrometer signals to changes in flow rate over the probe for liquid samples was assessed by preparing large samples of single inert gases dissolved in water and manually injecting these samples over the probe tip, while varying the flow rates from 0.4 to 10 ml/min.

The effects of inert-gas solubility on the mass spectrometer signal for each inert gas were assessed by comparisons of the signal for known inert-gas partial pressures in water, blood, and 20% Intralipid solution (Baxter Healthcare, Deerfield, IL). For SF_6, Kr, and DES, gas from a premixed tank with a known partial pressure of the inert gas in nitrogen was equilibrated with 30 ml of the liquid (water, rabbit blood from a pooled sample, or Intralipid) by adding 20 ml of gas in a 50-ml glass syringe, mixing, expelling the gas, and repeating the gas exchanges until the mass spectrometer signal for the liquid did not change with further exchanges. The 30 ml of liquid were then separated into 2- to 3-ml samples in 5-ml glass syringes, and the liquid samples were injected over the MMIMS probe at room temperature and in varied order. For ENF, DEE, and ACT, the inert "gas" was first diluted as a liquid into water, then 0.5 ml of the water and inert gas was added to 30 ml of the test liquid (water, rabbit blood from a pooled sample, or Intralipid), and 20 ml of air were added to the test liquid and equilibrated. The resulting inert-gas partial pressure in the test liquid was measured by head-space gas analysis, with comparison of the head-space gas mass spectrometer signal to the signal for a known inert-gas partial pressure from a premixed tank. The 30 ml of liquid were then separated into 2- to 3-ml samples in 5-ml glass syringes, and the liquid samples were injected over the MMIMS probe at room temperature and in varied order.

The ratio of mass spectrometer sensitivity for liquid-phase measurements to the sensitivity for gas-phase measurements was determined for each inert gas by preparing mixtures of ~35 ml of air, 15 ml of water, and a single inert gas in 50-ml glass syringes. The glass syringes were equilibrated by mechanical rotation in a temperature-controlled oven at 38°C for 1 h, and the gas and liquid phases were rapidly

separated into 50-ml gastight syringes (Hamilton, Reno, NV) and 5-ml glass syringes, respectively. The gas samples were injected over the MMIMS probe at room temperature, and the water samples were injected over the probe with the sample temperature maintained at 38°C with water-jacketed tubing.

Linearity of the mass spectrometer response for the gas phase was tested in 50-ml gastight syringes by serial dilutions of each inert gas in air. Linearity of the mass spectrometer response for the liquid phase was tested by serial dilutions of each inert gas in degassed water (distilled water that had been heated to boiling and then sealed in a syringe and cooled with no exposure to gas). Water samples for the liquid-phase serial dilutions were analyzed at room temperature.

Spectral overlap was assessed by flowing each single inert gas diluted in nitrogen over the probe, recording the current at the monitored peak for that gas, and recording the current at each of the other five peaks. The ratios of the current at each of the five peaks to the current at the monitored peak were used to construct the spectral overlap matrix **K,** which was subsequently used in all measurements for mixtures of the inert gases to convert the six measured currents to the six inert-gas partial pressures. The spectral overlap correction equation was

$$\mathbf{K} \times \mathrm{SP} = I \qquad (1)$$

where I is the vector of six measured currents at each peak (in the order of 127, 84, 101, 117, 59, and 58 amu), and SP is the vector of six products of sensitivity S $\times$ the inert-gas partial pressure P (in the order SF_6, Kr, DES, ENF, DEE, and ACT). The spectral overlap matrix used in *Eq. 1* was

$$\mathbf{K} = \begin{vmatrix} 1.0 & 0 & 0 & 0 & 0 & 0 \\ 0 & 1.0 & 0 & 0 & 0 & 0 \\ 0.012 & 0 & 1.0 & 0.104 & 0 & 0 \\ 0 & 0 & 0 & 1.0 & 0 & 0 \\ 0 & 0 & 0.015 & 0.014 & 1.0 & 0.088 \\ 0 & 0 & 0 & 0.002 & 0.048 & 1.0 \end{vmatrix}$$

Variability in the measurements of inert-gas partial pressures for a mixture of inert gases in blood samples was assessed in separate experiments in two New Zealand White rabbits after Institutional Animal Care and Use Committee approval of the experimental protocol. The rabbits were prepared as described below for the MIGET experiments. In one rabbit, a standard inert-gas infusate (see below for details) was infused at 80 ml/h for 2 h, and a 50-ml sample was taken from the pulmonary artery catheter in a single heparinized glass syringe. This single pulmonary arterial (PA) sample was divided into six samples of 2.5 ml in 5-ml glass syringes, and these blood samples were analyzed with the MMIMS probe with sample flow rate (1.0 ml/min by manual injection) and temperature control (water-jacketed tubing to keep the sample at 38°C at the probe tip) exactly matched to analyze conditions for the MIGET experiments. A schematic of the sample handling system and MMIMS inlet is shown in Fig. 1. Another six samples were taken from the pooled PA sample, and the measurements were repeated. In the second rabbit, to assess the effect of inert-gas partial pressure on variability of the measurement, the standard inert-gas mixture was infused at 27 ml/h for 1.5 h and then a single 40-ml PA sample was collected in a single glass syringe and divided into six samples of 2.5 ml in 5-ml syringes for analysis.

MIGET in normal rabbits. After Institutional Animal Care and Use Committee approval of the animal protocol, five female New Zealand White rabbits (3.5–4.3 kg) were anesthetized with 25 mg/kg of ketamine im and 5 mg/kg xylazine im. A 22-gauge catheter was placed in an ear vein, and normal saline was infused at 80 ml/h. Anesthesia was maintained with a continuous infusion of pentobarbital at 12 $mg \cdot kg^{-1} \cdot h^{-1}$ throughout the experiment. Rectal temperature was measured with a thermocouple probe and regulated to 38°C with a heating pad and lamp. A 3.5-mm endotracheal tube was placed via tracheostomy, and ventilation was controlled at a tidal volume of 25–30 ml and rate of 25 breaths/min (model 667, Harvard Apparatus, South Natick, MA). Grade 5 purity oxygen and grade 5 purity nitrogen (Air Products and Chemicals) were mixed to provide an inspired O_2 fraction of 0.75. Pancuronium (0.3 mg) was administered to facilitate controlled ventilation, and 0.1 $mg \cdot kg^{-1} \cdot h^{-1}$ was infused continuously throughout the experiment. A 20-gauge catheter was placed by cutdown in a femoral artery for continuous blood pressure measurement and arterial blood sampling. A 4-Fr catheter (angiographic balloon catheter, Arrow International, Reading, PA) was placed in the right external jugular vein by cutdown and positioned in the pulmonary artery with pressure waveform guidance. Airway pressures and systemic and PA blood pressures were transduced and recorded continuously. In preliminary experiments, analysis of arterial and mixed venous blood and mixed expired gas with the MMIMS system confirmed that there were no endogenous or exogenous sources of any inert gases in the absence of the inert-gas infusate.

A conical mixing chamber was added to the expiratory limb of the ventilator circuit, and the expiratory limb and mixing chamber were heated to 40–42°C to avoid water-vapor deposition and subsequent absorption of the soluble inert gases. Gas exiting the mixing chamber was shown to be well mixed by demonstration of no breath-to-breath time variance in CO_2 partial pressure with the use of a respiratory mass spectrometer (MGA-1100, Perkin-Elmer, Pomona, CA). Negligible loss of soluble inert gases to absorption in the expiratory limb was confirmed by use of a mechanical lung model that provided a constant partial pressure of ACT (394

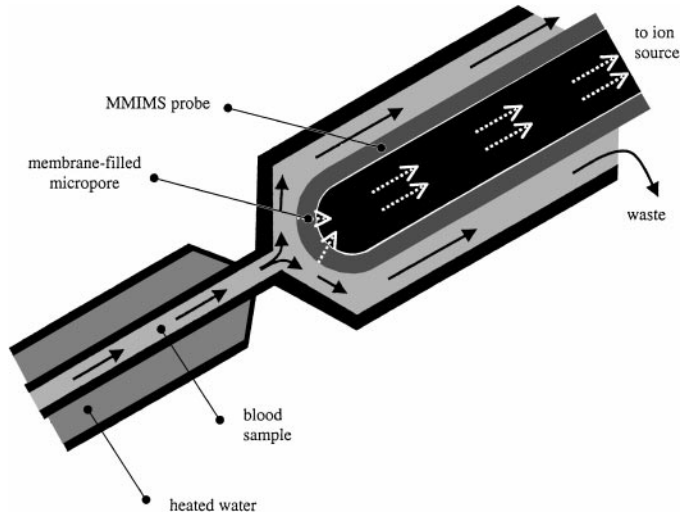

Fig. 1. Schematic cutaway of the micropore membrane inlet mass spectrometry (MMIMS) probe tip and the channel of blood flowing over the membrane-filled pores at the probe tip. Blood (black arrows) is delivered to the probe in water-jacketed tubing to maintain blood sample temperature at 38°C. The inert gases (white dotted arrows) permeate through the membranes in pores at the probe tip and into the vacuum system (black area) where they diffuse to the mass spectrometer ion source.

parts/million ACT) in nitrogen and saturated water vapor at 40°C. When the lung model was mechanically ventilated and gas samples were taken directly from the lung and from the mixed expired port distal to the mixing chamber, dead space calculated from the ACT partial pressures matched known dead spaces inserted into the mechanical lung model within 3%. The outlet of the mixing chamber was placed under 2.5 cmH_2O of positive end expiratory pressure. For each experiment, the minute ventilation was measured directly with a bell spirometer (Warren Collins, Boston, MA) attached to the expiratory limb.

The inert-gas infusate was prepared by equilibrating 5% Kr-95% SF_6 with 250 ml of normal saline and then ejecting the excess gas and adding the rest of the inert "gases" as liquids: 150 μl DES, 170 μl ENF, 0.5 ml DEE, and 2.7 ml ACT. After placement of the endotracheal tube and all catheters and confirmation of stable hemodynamics for at least 30 min, the saline infusion was discontinued, and the inert gases dissolved in saline were infused at 80 ml/h. After 40 min of inert-gas infusion, the first set of systemic arterial, PA, and mixed expired samples for MIGET were collected simultaneously. A second set of samples was taken 30 min later, and a third set was taken 30 min after that. Additional arterial and PA blood samples (1.0 ml each) were taken with each set of MIGET samples for blood-gas analysis and measurement of hematocrit.

The blood samples for MIGET (2.0–2.5 ml each for arterial and PA samples) were collected in heparinized 5-ml glass syringes and were placed in a 38°C oven until analysis. Samples were injected manually over the MMIMS probe tip at 1.0 ml/min within 30 min of collection (Fig. 1). Blood temperature at the probe tip was maintained at 38°C with water-jacketed tubing. Mixed expired gas samples (30–35 ml) were collected in 50-ml gastight syringes (Hamilton). Mixed expired samples were analyzed at room temperature (21–24°C).

The mixed expired gas sample was analyzed first for each set of MIGET samples, followed by the arterial sample, followed by the PA sample. The inert gases were analyzed in the order SF_6, DES, ENF, Kr, DEE, and ACT.

The measurements of ion currents at six different amu were converted to retention and excretion data. First, vacuum system background (negligible for all gases except DEE, for which background was ~50% of the signal) was subtracted from the measured current at each amu. Next, spectral overlap was corrected for by using *Eq. 1*, giving a product of mass spectrometer S × P for each inert gas. Retention (systemic arterial inert-gas partial pressure/$P\bar{v}$) was then calculated from the ratio of arterial and mixed venous SP products, with the S factoring out. Next, the data for the ratio of gas-phase sensitivity to liquid-phase sensitivity were used to convert the SP product for the mixed expired gas measurements to an equivalent SP product for the liquid phase. Finally, excretion (mixed expired inert-gas partial pressure/$P\bar{v}$) was calculated from the ratio of the mixed expired equivalent SP to the mixed venous SP, again with the S factoring out.

In a separate set of experiments, partition coefficients for each of the inert gases in rabbit blood were measured by using the double-dilution method (38). First, the validity of the gas extraction/double dilution method by using the MMIMS system for analysis of gas partial pressures in the equilibrated gas phase was established by repeated measurements of the inert-gas solubilities in samples of distilled water. Each of the six inert gases was individually added to measured volumes of water and equilibrated with a measured volume of air at 38°C. The gas phase was separated from the liquid phase, and a second measured volume of air was equilibrated with the water sample. Initial and final inert-gas partial pressures in the gas phase were measured with the MMIMS probe. Forty-milliliter blood samples were then collected from six female New Zealand White rabbits (3.7–4.9 kg). The inert-gas solubilities were measured for each rabbit by the double-dilution method, matching the technique established for the distilled water experiments, with the modification that a 5% CO_2-air mixture was used for the equilibration gas.

Retention and excretion data and measured inert-gas solubilities were transformed into $\dot{V}_A/\dot{Q}$ distributions by using algorithms derived by Evans and Wagner (9). Input data for the $\dot{V}_A/\dot{Q}$ transformations included the measured retention data for each set of samples, the measured excretion data for each set of samples, measured partition coefficients for the inert gases in rabbit blood, minute ventilation measured for each rabbit, cardiac output for each set of samples derived from the Fick principle for each inert gas, with a weighted average as described by Wagner and Lopez (37), and weighting factors based on variance estimates for each retention measurement, as derived from the data on repeated measurements from the pooled PA samples.

RESULTS

Inert-gas partial pressures in gas and liquid samples. The mass spectrometer signals for SF_6, Kr, DES, and ENF all reached at least 98% of their steady-state levels within 30 s after a step change for the liquid and gas samples. The mass spectrometer signals for DEE and ACT reached 90–95% of their steady-state signal within 30 s and then, more slowly, reached at least 98% of their steady-state values within 120 s for the liquid and gas samples. The slow component of the time response for DEE and ACT was also present after a step decrease in gas partial pressure, with complete return to baseline for all gases within 4 min after exposure of the probe tip to zero partial pressures of the inert gases.

Increases in the sample flow above the normal rate of 1.0 ml/min resulted in no detectable change in the mass spectrometer signal for any gas, up to a sample flow of 10 ml/min. Decreases in sample flow to 0.4 ml/min resulted in <9% decrease in signal for all gases.

Figure 2 shows the mass spectrometer signal for each inert gas dissolved in water, a pooled blood sample from normal rabbits, and 20% Intralipid solution, at the same inert-gas partial pressure. The signal for SF_6 in lipid was significantly different from the signals for water and blood ($P = 0.006$ by one-way ANOVA with Student-Newman-Keuls post hoc testing), with a ratio for the lipid/water signals of 1.12. The signal for ENF in lipid was significantly different from the signal for blood ($P = 0.037$ by one-way ANOVA with Student-Newman-Keuls post hoc testing), with a ratio for lipid/blood signals of 1.06. No other differences in signals for water, blood, and lipid were statistically significant.

The ratio of mass spectrometer sensitivity for liquid-phase measurements to the sensitivity for gas-phase measurements is shown in Table 1 (means ± SD). All inert-gas partial pressures were either approximately in the range of, or severalfold larger than, typical

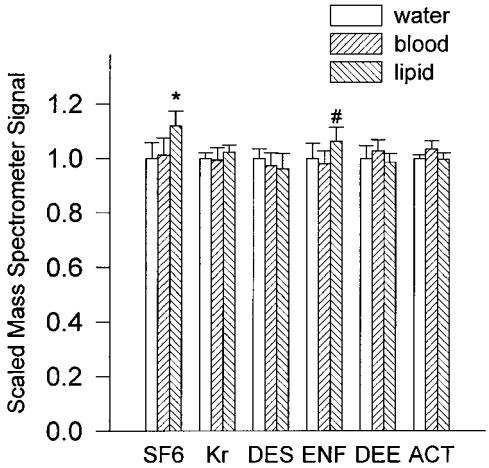

Fig. 2. Independence of mass spectrometer signal from variations in inert-gas solubility in liquid samples [water, a pooled blood sample from normal rabbits, and 20% Intralipid solution (lipid)]. For each gas [sulfur hexafluoride (SF_6), krypton (Kr), desflurane (DES), enflurane (ENF), diethyl ether (DEE), and acetone (ACT)], the mass spectrometer signals are normalized to the signal for water. All inert-gas partial pressures are either approximately in the range of, or severalfold larger than, typical partial pressures in a pulmonary arterial sample in the rabbit experiments. Data plotted are means ± SD for $n = 6$ rabbits. Significant difference compared with signals for *water and blood and #blood, $P < 0.05$.

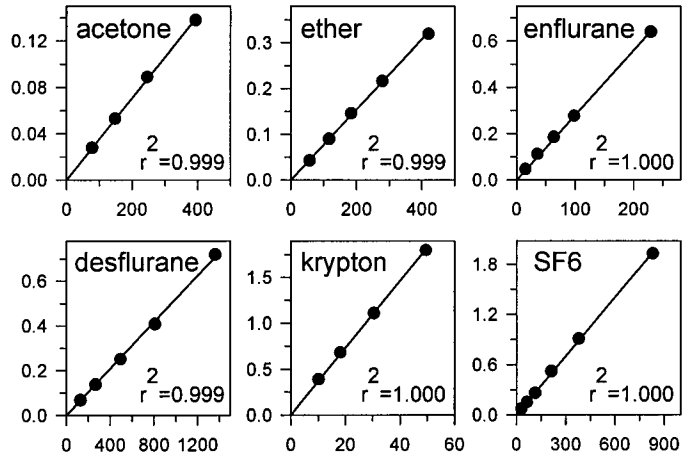

Fig. 3. Linearity of MMIMS system for the inert gases in gas phase. The *x*-axis shows inert-gas partial pressure in parts/million; *y*-axis shows mass spectrometer output current in A × 10^{10}. Data were fitted with forced linear regression through the origin.

partial pressures for PA samples in the rabbit experiments.

Linearity of mass spectrometer signal vs. gas partial pressure for measurements in the gas phase is shown in Fig. 3, where the upper range of gas partial pressure for each plot exceeds the partial pressures for typical mixed expired samples in the rabbit experiments. Linearity of mass spectrometer signal vs. gas partial pressure for measurements in the liquid phase is shown in Fig. 4, where the upper range of signal for each plot exceeds the mass spectrometer signals for typical mixed venous samples in the rabbit experiments.

Coefficients of variation (SD/mean) for repeated measurements of inert-gas partial pressures in pooled rabbit blood samples are shown in Table 2.

MIGET in normal rabbits. Table 3 presents hemodynamic and arterial blood-gas data for the rabbit experiments.

The retention and excretion data for all five rabbits are shown in Fig. 5. The mean values for retention and excretion for each rabbit are shown in Fig. 6. Each set of retention and excretion data required 4–5 ml of blood, and the analysis time for a complete retention and excretion set was ~8 min.

Solubilities of the inert gases in water at 38°C (ml gas at 38°C, in standard atm·ml $water^{-1}$·atm^{-1}) were SF_6, 0.00378 ± 0.00062 (SD); Kr, 0.0509 ± 0.0036; DES, 0.287 ± 0.027; ENF, 0.758 ± 0.071; DEE, 14.6 ± 1.0; and ACT 318 ± 35 ($n = 8$ measurements). Solubilities of the inert gases in rabbit blood at 38°C (ml gas at 38°C, in standard atm·ml $blood^{-1}$·atm^{-1}) were SF_6, 0.00812 ± 0.0010 (SD); Kr, 0.0522 ± 0.0062; DES, 0.623 ± 0.051; ENF, 2.34 ± 0.17; DEE, 11.8 ± 0.87; and ACT 309 ± 38 ($n = 6$ measurements).

The three sequential sets of $\dot{V}_A/\dot{Q}$ distributions for one of the rabbits are shown in Fig. 7. A summary of the mean $\dot{V}_A/\dot{Q}$ data for each rabbit is presented in Table 4. Fourteen of 15 data sets had a residual sum of squares (RSS) of <16.8 (30). The first set in *rabbit 4* had a RSS of 42.2, likely related to the obvious error in mixed expired measurement of DEE (Fig. 5), and this

Table 1. *Ratio of mass spectrometer sensitivities for liquid-phase and gas-phase measurements*

Inert Gas	Liquid/Gas Sensitivity
Sulfur hexafluoride	0.248 ± 0.013
Krypton	0.535 ± 0.007
Desflurane	0.568 ± 0.069
Enflurane	0.382 ± 0.012
Diethyl ether	0.592 ± 0.042
Acetone	0.933 ± 0.065

Values are means ± SD. Liquid/gas, ratio of liquid phase to gas phase.

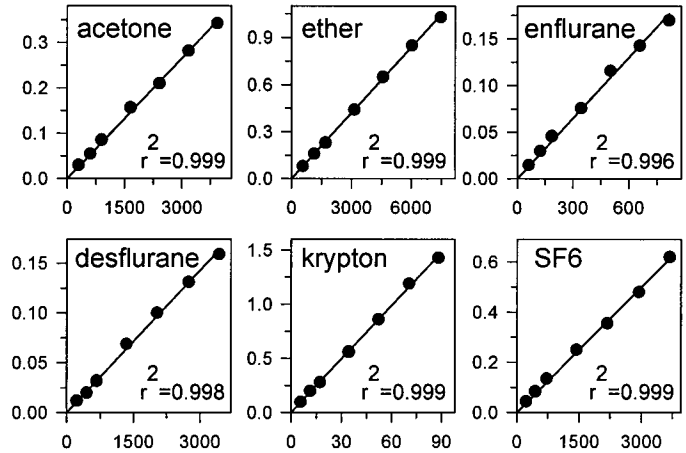

Fig. 4. Linearity of MMIMS system for the inert gases in liquid phase. The *x*-axis shows inert-gas partial pressure in parts/million; *y*-axis shows mass spectrometer output current in A × 10^{10}. Data were fitted with forced linear regression through the origin.

Table 2. *Variability of measurements of inert-gas tensions in rabbit blood samples*

Inert Gas	PA1	PA2	PA-Low
Sulfur hexafluoride	0.0563	0.0693	0.0834
Krypton	0.0159	0.0446	0.0147
Desflurane	0.0667	0.0678	0.0406
Enflurane	0.0446	0.0401	0.0829
Diethyl ether	0.0549	0.0547	0.0549
Acetone	0.0376	0.0381	0.0552

All values are coefficients of variation (SD/mean) for 6 repeated measurements of inert-gas tensions in the same blood samples. PA, pulmonary arterial. One typical pooled mixed venous sample was analyzed twice (PA1 and PA2). A second pooled mixed venous sample (PA-Low) had lower inert-gas partial pressures than typically encountered in the rabbit experiments.

set was not included in the mean data of Table 4. All 14 of the 15 $\dot{V}_A/\dot{Q}$ distributions with acceptable RSS were unimodal.

DISCUSSION

Applications of MIGET have been primarily limited to research settings in adult humans and large animals, with very few studies in small animals and no real-time use in clinical care of patients. Although MIGET provides detailed and unique information on pulmonary $\dot{V}_A/\dot{Q}$ distributions and pathophysiology, the large blood sample volume, long analysis time, and highly technical labor required for traditional MIGET by GC have restricted the widespread adoption of the technique. MIMS has been applied before to MIGET to overcome some of these limitations, with one description of initially promising results but no further reports of this approach (23).

One problem common to early MIMS systems was very slow time responses and vacuum system memory effects for certain analytes. Although not specifically reported by Mastenbrook et al. (23), the configuration of their tubing between the membrane and the mass spectrometer inlet, as well as the variability they reported for their ACT measurements, suggests that this was a problem for this early MIMS system. Very slow time responses and vacuum system memory effects are now understood to be the result of tight adsorption of certain analytes to the walls of the vacuum system and subsequent slow release (20). We minimized these effects by keeping the length of stainless steel tubing between the membrane and the ion source as short as possible and by heating the inlet, the vacuum system, and the connection tubing. The small slow component of our system's time response for ACT and DEE, observed with step increases and step decreases in gas partial pressure, was likely due to these effects. Avoidance of long sections of unheated tubing between the membrane and the ion source, however, kept these effects within tolerable limits.

Another important limitation of prior MIMS systems has been the stirring effect, which refers to the difference in signal between stagnant liquid and rapidly flowing liquid (12). Stirring effect is a consequence of resistance to diffusion in the liquid boundary layer near the membrane and is a function of the permeability (product of diffusivity and solubility) of the inert gas in the liquid vs. the inert-gas permeability in the membrane. For a MIMS system with significant stirring effect, the mass spectrometer signal is dependent not only on the inert-gas partial pressure in the liquid, but also on the inert-gas solubility and diffusivity in the liquid sample, as well as the flow field in the vicinity of the membrane. The MIMS system applied by Mastenbrook et al. had significant stirring effect (4), and these investigators successfully overcame the resulting flow dependence by using a reproducible flow field near the membrane (23). This approach, however, did not eliminate the solubility dependence of the mass spectrometer signal.

Stirring effect and its resulting flow dependence and solubility dependence can be eliminated entirely in MIMS systems by use of thick membranes, which increase the membrane diffusional resistance relative to the diffusional resistance of the liquid sample. Thick membranes, however, lead to unacceptably long time responses because of the dependence of membrane time response on the square of membrane thickness (42).

MMIMS offers a solution to this dilemma. In MMIMS, confinement of the membrane to a small pore results in both a rapid time response and minimal stirring effect. The rapid time response is a consequence of the use of very thin membranes in MMIMS. The reductions in stirring effect are thought to be the result of the three-dimensional diffusion profiles in the liquid near the membrane (1). The inert-gas concentration profiles in the liquid around a pore that approximates a point with nearly zero area are expected, on the basis of symmetry, to be hemispherical, whereas the concentration profiles within the membrane are expected to be approximately planar. Consequently, the area available for diffusion in the membrane should be much smaller than the area available for

Table 3. *Hemodynamic, arterial blood pH, and gas tension data*

	Sample 1	*Sample 2*	*Sample 3*
HR, beats/min	232 ± 29	257 ± 34*	280 ± 35*
MAP, mmHg	91 ± 3	103 ± 6*	110 ± 7*
Ppa, mmHg	12.3 ± 1.3	12.7 ± 1.0	14.6 ± 1.6*,†
Ppad, mmHg	8.0 ± 1.9	8.2 ± 1.3	9.4 ± 1.7
Pa_{O_2}, Torr	306 ± 92	326 ± 31	286 ± 37
Pa_{CO_2}, Torr	29.1 ± 7.4	28.6 ± 3.6	25.9 ± 1.6
pH_a	7.37 ± 0.04	7.35 ± 0.06	7.34 ± 0.06
Hct, %	26.0 ± 4.5	27.1 ± 4.7	25.2 ± 4.0

Values are means ± SD for $n = 5$ subjects, measured before each set of blood samples for multiple inert-gas elimination technique. HR, heart rate; MAP, mean arterial pressure; Ppa, mean pulmonary arterial pressure; Ppad, pulmonary arterial diastolic pressure; Pa_{O_2}, arterial oxygen tension; Pa_{CO_2}, arterial carbon dioxide tension; pH_a, arterial pH; Hct, hematocrit. *Different from *sample 1*, $P < 0.05$ (repeated-measures ANOVA with Student-Newman-Keuls post hoc testing); †different from *sample 2*, $P < 0.05$ (repeated measures ANOVA with Student-Newman-Keuls post hoc testing).

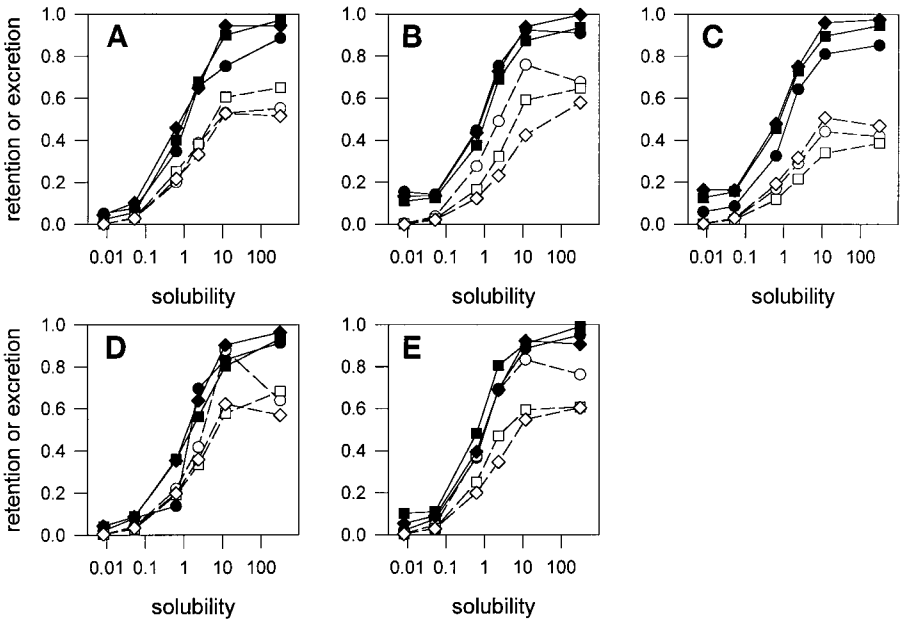

Fig. 5. Retention (solid symbols) and excretion (open symbols) data in each subject [*subjects 1–5* (*A–E*, respectively)], for the first set (circles), second set (squares), and third set (diamonds). Solubilities are Ostwald coefficients in ml gas at body temperature, standard atm/ml blood-atm.

diffusion in the liquid, thereby increasing the resistance to diffusion in the membrane vs. the liquid. The pore size cannot be reduced without limit, because reductions in membrane area also reduce the sensitivity of the system (mass spectrometer current/gas partial pressure). The data in Figs. 1–3 and Table 2, however, suggest that, with a sensitive mass spectrometer, the pore area can be small enough to substantially reduce stirring effect and still have enough sensitivity for accurate measurement. In our system, we restored some sensitivity by the use of multiple pores. For several micropores functioning independently, it is expected that sensitivity will increase linearly with the number of pores, but the system time response and stirring effect for a population of pores should be approximately independent of the number of pores.

The insensitivity of the mass spectrometer signal to changes in sample flow over the probe tip is a consequence of the small stirring effect for the MMIMS probe. Although our system did have some flow dependence at low flows for some of the gases (most noticeably SF_6 and ENF), the undetectable changes in signal with increases in flow to rates >1.0 ml/min indicate that sample flows of 1.0 ml/min were adequate to overcome the small amount of stirring effect from the MMIMS probe.

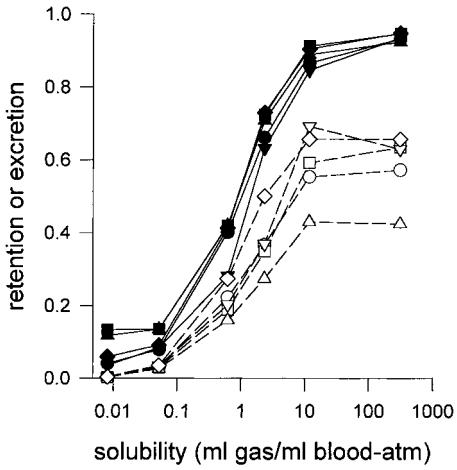

Fig. 6. Means of the 3 sets of retention (solid symbols) and excretion (open symbols) data for *subjects 1* (circles), *2* (squares), *3* (triangles), *4* (inverted triangles), and *5* (diamonds).

In addition to insensitivity to sample flow, the small stirring effect for the MMIMS probe results in insensitivity to variations in inert-gas solubility in the sample, as shown in Fig. 2. Solubility of inert gases in blood samples is known to vary from subject to subject, due primarily to variations in blood protein content and blood lipid content (22, 38). Therefore, even for a subject in which the inert-gas solubilities are at the lowest values in the distribution of solubilities for a population of subjects, the inert-gas solubilities in water are expected to be lower. Similarly, inert-gas solubilities in 20% Intralipid solution are expected to be larger than any of the highest values in blood encountered in any individual subject. Even for these extremes in values of solubility for water and 20% Intralipid, the variations of mass spectrometer signal with solubility shown in Fig. 1 are <12% for SF_6, <6% for ENF, and insignificant for the other gases.

Although the mass spectrometer signal is minimally dependent on the gas solubility in the liquid sample, the signal does depend on whether the sample is gas or liquid (Table 1). The difference in sensitivity for gas-phase measurements vs. liquid-phase measurements may be in part due to temperature dependence of permeation through the membrane and may be due in part to swelling effects in the silicone membrane. Membrane temperature for the blood samples is expected to equal the blood sample temperature at 38°C. The gas samples, however, are injected at room temperature. The membrane temperature for the gas samples in our

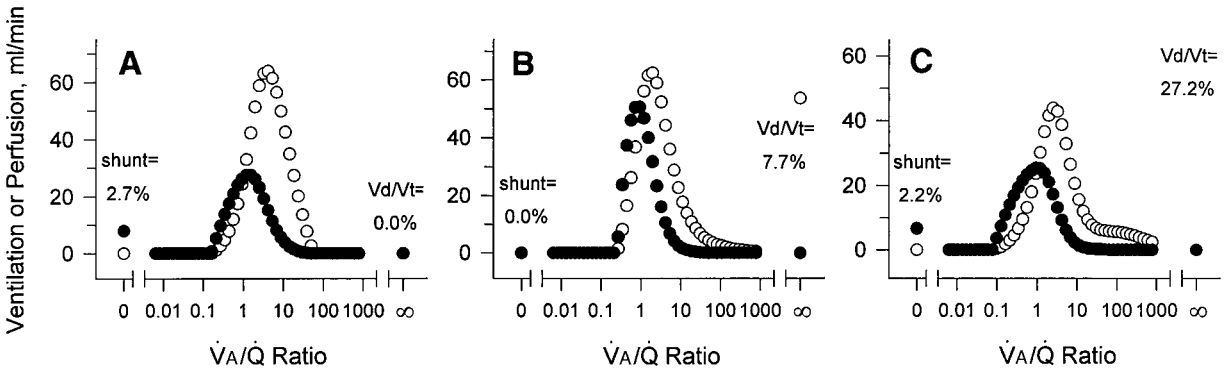

Fig. 7. The 3 sequential ventilation-to-perfusion ratio ($\dot{V}_A/\dot{Q}$) distributions for the first subject. *A–C*: *sets 1–3*, respectively. ●, $\dot{Q}$; ○, $\dot{V}_A$. V_D/V_T, ratio of dead space volume to tidal volume (expressed as $\%V_T$).

present system, determined by the balance between heat losses to the gas surrounding the probe and heat conducted along the probe tubing from the heated ion source, is ~30°C. Membrane temperature affects both the solubility and the diffusivity of the inert gases in the membrane (5) and, therefore, is expected to influence sensitivity. Silicone membranes are also known to expand slightly when immersed in aqueous samples (21), a phenomenon known as swelling, and membrane swelling is known to affect the permeability of polymer membranes for most gases (21, 25). Further work will be required to assess the relative contributions of each of these mechanisms.

The MMIMS system rapidly provides direct measurements of inert-gas partial pressures in small blood samples, with no extraction into a gas phase, and minimal dependence on inert-gas solubility in blood. In this report, we have applied MMIMS to MIGET and determination of pulmonary $\dot{V}_A/\dot{Q}$ distributions, but there are other applications in physiology in which these features could be advantageous, such as the estimation of tissue blood flow (16) and determinations of heterogeneity of perfusion-to-volume ratios in tissue (13).

Any six inert gases can be used for MIGET, provided that the gas solubilities in blood cover a wide range of solubilities and are reasonably evenly distributed within that range of solubilities (40). We used six inert gases similar to the series reported by Mastenbrook et al. (23), and the spectral overlap matrix **K** in *Eq. 1* indicates very little overlap, with the largest being the current at the DES of 101 amu of 10.4% of the ENF current and the current at the DEE of 59 amu of 8.8% of the ACT current.

The variability in the MMIMS method shown in Table 2 is greater than the variability reported for

Table 4. *Summary of $\dot{V}_A/\dot{Q}$ distributions*

	Subject No.				
	1	*2*	*3*	*4*	*5*
Residual sum of squares	4.40 ± 3.31	4.25 ± 2.08	5.12 ± 2.61	3.05 ± 1.47	8.05 ± 7.25
		Flow distribution			
CO	366 ± 34	345 ± 112	276 ± 86	334 ± 62	431 ± 126
Shunt	1.6 ± 1.4	8.6 ± 0.4	8.2 ± 3.3	3.0 ± 0.4	2.7 ± 1.9
Low $\dot{V}_A/\dot{Q}$	0.4 ± 0.7	0.0 ± 0.0	0.0 ± 0.0	0.7 ± 0.9	0.0 ± 0.0
Normal $\dot{V}_A/\dot{Q}$	96.2 ± 2.5	90.4 ± 1.1	89.5 ± 1.3	91.9 ± 3.9	96.6 ± 2.3
High $\dot{V}_A/\dot{Q}$	1.8 ± 1.1	1.0 ± 1.1	2.3 ± 2.3	4.4 ± 3.3	0.7 ± 1.0
Mean $\dot{V}_A/\dot{Q}_Q$	1.12 ± 0.27	1.17 ± 0.20	1.21 ± 0.40	1.44 ± 0.23	0.93 ± 0.12
Log SD_Q	0.95 ± 0.14	0.79 ± 0.09	0.90 ± 0.18	1.11 ± 0.25	0.79 ± 0.12
		Ventilation distribution			
$\dot{V}_E$	715 ± 0.0	657 ± 0.0	602 ± 0.0	706 ± 0.0	650 ± 0.0
Low $\dot{V}_A/\dot{Q}$	0.0 ± 0.0	0.0 ± 0.0	0.0 ± 0.0	0.0 ± 0.0	0.0 ± 0.0
Normal $\dot{V}_A/\dot{Q}$	71.7 ± 13.2	52.1 ± 8.5	53.6 ± 10.1	65.0 ± 7.8	78.5 ± 18.4
High $\dot{V}_A/\dot{Q}$	16.6 ± 4.5	10.4 ± 9.8	19.3 ± 18.0	31.2 ± 13.1	12.1 ± 17.2
Dead space	11.6 ± 14.0	30.5 ± 24.7	27.1 ± 24.2	3.9 ± 5.4	9.4 ± 16.3
Mean $\dot{V}_A/\dot{Q}_V$	3.77 ± 0.86	3.26 ± 1.82	4.99 ± 2.95	6.29 ± 2.21	3.14 ± 2.55
Log SD_V	1.32 ± 0.31	1.18 ± 0.39	1.35 ± 0.47	1.36 ± 0.17	1.24 ± 0.56

Values for each subject are means ± SD for 3 measurements. $\dot{V}_A/\dot{Q}$, ventilation-to-perfusion ratio. CO is the weighted cardiac output from the retention/excretion data in ml/min. Shunt, low $\dot{V}_A/\dot{Q}$, normal $\dot{V}_A/\dot{Q}$, and high $\dot{V}_A/\dot{Q}$ for the flow distribution are all given as percentages of CO. Low $\dot{V}_A/\dot{Q}$ is the range $0 < \dot{V}_A/\dot{Q} \leq 0.1$. Normal $\dot{V}_A/\dot{Q}$ is the range $0.1 < \dot{V}_A/\dot{Q} \leq 10$. High $\dot{V}_A/\dot{Q}$ is the range $10 < \dot{V}_A/\dot{Q} < \infty$. Mean $\dot{V}_A/\dot{Q}_Q$ is the mean $\dot{V}_A/\dot{Q}$ value for the perfusion distribution. Log SD_Q is the second moment of the perfusion distribution. $\dot{V}_E$ is minute ventilation in ml/min. Low $\dot{V}_A/\dot{Q}$, normal $\dot{V}_A/\dot{Q}$, high $\dot{V}_A/\dot{Q}$, and dead space for the ventilation distribution are all given as percentages of $\dot{V}_E$. Mean $\dot{V}_A/\dot{Q}_V$ is the mean $\dot{V}_A/\dot{Q}$ value for the ventilation distribution. Log SD_V is the second moment of the ventilation distribution.

traditional MIGET by GC analysis. Wagner et al. (38), for example, reported coefficients of variation for repeated measurements of inert-gas partial pressures in a pooled blood sample of 6% for SF_6 and <3% for the other inert gases in their MIGET series. It is anticipated that the precision of the MMIMS method will continue to improve with further refinements, particularly the use of micromachining techniques to substantially increase the number of pores and more rigorous control of the membrane temperature for the analysis of the mixed expired samples.

The hemodynamic and arterial blood-gas data shown in Table 3 illustrate the stability of the animal preparation. The gradual increase in heart rate, mean arterial pressure, and PA pressure over time may have been a result of progressive sympathetic stimulation from the continuous infusion of pancuronium (8). There was no evidence, as indicated by the pulmonary artery diastolic pressures, of volume overload from the inert-gas infusate in any rabbit. The stability of the hematocrit over time suggests that the amount of blood volume sampled for MIGET in this small animal model was well tolerated. The blood sample volume for this MMIMS system was 2 ml/sample or 4 ml per set of retention and excretion data (2 ml each for the mixed venous and arterial samples). The amount of inert gas sampled into the mass spectrometer is a very small fraction of the inert gases in 2 ml of blood, and it is possible that future improvements in probe temperature control, sample flow control, and the precision of the flow channel at the probe tip in Fig. 1 could lead to even smaller blood sample volumes in future MMIMS systems.

The inspired gases were mixed from purified oxygen and nitrogen to eliminate the trace level Kr that can be commonly found in oxygen tanks. Although it is possible to carry out MIGET accurately in the presence of a stable background of exogenous Kr (30), for this experimental protocol we used purified gases to avoid any corrections for environmental background.

Because the MMIMS technique measures inert-gas partial pressures in blood samples with minimal dependence on the inert-gas solubility in blood, the accuracy of the retention and excretion data in Figs. 5 and 6 is unaffected by variations in inert-gas solubilities within and between subjects. Values for solubility are required, however, for transforming the retention and excretion data into $\dot{V}_A/\dot{Q}$ distributions. The data in Fig. 7 and Table 4 were calculated by using measurements of the population means for the inert-gas solubilities in rabbit blood and do not account for variations in solubilities between individual subjects. The acceptable RSS in 14 of 15 data sets (30) suggests that this approach provided reasonable accuracy for recovery of $\dot{V}_A/\dot{Q}$ distributions in normal rabbits. In general, however, the RSS in Table 4 are larger than values that have been reported for the traditional GC approach to MIGET in experienced hands (14). The relatively large RSS in our experiments could reflect either the variability in the partial pressure measurements with MMIMS or errors in solubility as a result of individual variations around the population mean.

The small blood sample volume and rapid analysis time for measurement of inert-gas partial pressures by MMIMS could be used to the greatest advantage in studies in which gas exchange and $\dot{V}_A/\dot{Q}$ distributions are changing rapidly but solubility remains constant over the course of an experiment. For example, MIGET by MMIMS could be used in a small-animal model to measure sequential changes in $\dot{V}_A/\dot{Q}$ distributions in response to therapeutic interventions, and a large blood sample volume could be collected at the end of the experiment for measurement of inert-gas solubilities by established methods (31, 38).

The mean second moment of the perfusion distribution (log $SD_{\dot{Q}}$) for the rabbit $\dot{V}_A/\dot{Q}$ distributions was 0.91, comparable to the values of 0.91, 0.85, 0.78, and 0.94 for normal rabbits reported by Lagerstrand and Hedenstierna (19). These $\dot{V}_A/\dot{Q}$ distributions are broad compared with anesthetized, ventilated normal dogs [log $SD_{\dot{Q}}$ of 0.55 (35), 0.45 (10), and 0.68 (17)] and normal humans [log $SD_{\dot{Q}}$ of 0.43 (36)]. Also, the ventilation distribution was right-shifted toward high $\dot{V}_A/\dot{Q}$ units with a mean $\dot{V}_A/\dot{Q}$ value for ventilation distribution (mean $\dot{V}_A/\dot{Q}_{\dot{V}}$) of 3.77, which is also comparable to the value of 2.65 reported by Lagerstrand and Hedenstierna (19). These ventilation distributions are substantially right-shifted compared with anesthetized, ventilated normal dogs [mean $\dot{V}_A/\dot{Q}_{\dot{V}}$ of 1.03 (17)] and normal humans [mean $\dot{V}_A/\dot{Q}_{\dot{V}}$ of 1.10 (36)]. The reasons for comparatively broad $\dot{V}_A/\dot{Q}$ distributions in the rabbit are not clear, but a broad $\dot{V}_A/\dot{Q}$ distribution in a small lung with limited gravitational variation supports the evidence that factors other than gravity play a substantial role in $\dot{V}_A/\dot{Q}$ heterogeneity (17). Right-shifted $\dot{V}_A/\dot{Q}$ distributions have been reported in sheep when tidal volumes are relatively large, which is thought to be due to overdistention of parts of the lung and reductions in blood flow to those regions (30). Alternatively, high $\dot{V}_A/\dot{Q}$ regions could be a consequence of exchange of the highly soluble gases in the conducting airways (32).

In summary, the unique combination of rapid response time and minimal stirring effect provided by MMIMS resulted in a system for the rapid, direct measurement of inert-gas partial pressures in small blood samples, with minimal dependence on the solubility of the inert gas in blood. The blood-sample volume for a complete set of retention and excretion data for MIGET was 4–5 ml, and analysis time for a single $\dot{V}_A/\dot{Q}$ determination was ~8 min. This new approach for MIGET has potential to make determinations of $\dot{V}_A/\dot{Q}$ distributions more widely available in research applications in small animal models.

The authors gratefully acknowledge Dr. Peter D. Wagner for supplying the computer program for the $\dot{V}_A/\dot{Q}$ transformations.

This study was funded in part by National Heart, Lung, and Blood Institute Grants R41-HL-59052 and HL-09040; by SpectruMedix Corporation, State College, PA; and by the University of Pennsylvania Research Foundation.

REFERENCES

1. **Baumgardner JE, Quinn JA, and Neufeld GR.** Micropore membrane inlet mass spectrometer probes suitable for measurement of tissue surface gas tensions. *J Mass Spectrom* 30: 563–571, 1995.
2. **Beydon L, Cinotti L, Rekik N, Radermacher P, Adnot S, Meignan M, Harf A, and Lemaire F.** Changes in the distribution of ventilation and perfusion associated with separation from mechanical ventilation in patients with obstructive pulmonary disease. *Anesthesiology* 75: 730–738, 1991.
3. **Bier ME and Cooks RG.** Membrane interface for selective introduction of volatile compounds directly into the ionization chamber of a mass spectrometer. *Anal Chem* 59: 597–601, 1987.
4. **Brantigan JW, Gott VL, Vestal ML, Fergusson GJ, and Johnston WH.** A nonthrombogenic diffusion membrane for continuous in vivo measurement of blood gases by mass spectrometry. *J Appl Physiol* 28: 375–377, 1970.
5. **Crank J.** *Diffusion in Polymers*. New York: Academic, 1968.
6. **Dantzker DR, Brook LJ, Dehart P, Lynch JP, and Weg JG.** Ventilation-perfusion distributions in the adult respiratory distress syndrome. *Am Rev Respir Dis* 120: 1039–1052, 1979.
7. **Dantzker DR and D'Alonzo GE.** The effect of exercise on pulmonary gas exchange in patients with severe chronic obstructive pulmonary disease. *Am Rev Respir Dis* 134: 1135–1139, 1986.
8. **Docherty JR and McGrath JC.** Sympathomimetic effects of pancuronium bromide on the cardiovascular system of the pithed rat: a comparison with the effects of drugs blocking the neuronal uptake of noradrenaline. *Br J Pharmacol* 64: 589–599, 1978.
9. **Evans JW and Wagner PD.** Limits on $\dot{V}A/\dot{Q}$ distributions from analysis of experimental inert gas elimination. *J Appl Physiol* 42: 889–898, 1977.
10. **Frans A, Clerbaux T, Willems E, and Kreuzer F.** Effect of metabolic acidosis on pulmonary gas exchange of artificially ventilated dogs. *J Appl Physiol* 74: 2301–2308, 1993.
11. **Gea J, Roca J, Torres A, Agusti AG, Wagner PD, and Rodriguez-Roisin R.** Mechanisms of abnormal gas exchange in patients with pneumonia. *Anesthesiology* 75: 782–789, 1991.
12. **Gronlund J, Johansen O, and Jensen B.** New transcutaneous P_{O_2} probe based on mass spectrometry with low stirring effect. *Med Biol Eng Comput* 23: 254–257, 1985.
13. **Gronlund J, Malvin GM, and Hlastala MP.** Estimation of blood flow distribution in skeletal muscle from inert gas washout. *J Appl Physiol* 66: 1942–1955, 1989.
14. **Hachenberg T, Tenling A, Hansson HE, Tyden H, and Hedenstierna G.** The ventilation-perfusion relation and gas exchange in mitral valve disease and coronary artery disease. *Anesthesiology* 86: 809–817, 1997.
15. **Hlastala MP.** Multiple inert gas elimination technique. *J Appl Physiol* 56: 1–7, 1984.
16. **Hoeft A, Sonntag H, Stephan H, and Kettler D.** The influence of anesthesia on myocardial oxygen utilization efficiency in patients undergoing coronary bypass surgery. *Anesth Analg* 78: 857–866, 1994.
17. **Kallas HJ, Domino KB, Glenny RW, Anderson EA, and Hlastala MP.** Pulmonary blood flow redistribution with low levels of positive end-expiratory pressure. *Anesthesiology* 88: 1291–1299, 1998.
18. **Kotiaho T, Lauritsen FR, Choudhury TK, Cooks RG, and Tsao GT.** Membrane introduction mass spectrometry. *Anal Chem* 63: 875A–883A, 1991.
19. **Lagerstrand L and Hedenstierna G.** Gas-exchange impairment: its correlation to lung mechanics in acute airway obstruction (studies on a rabbit asthma model). *Clin Physiol* 10: 363–380, 1990.
20. **Lauritsen FR.** A new membrane inlet for on-line monitoring of dissolved, volatile organic compounds with mass spectrometry. *Int J Mass Spec Ion Proc* 95: 259–268, 1990.
21. **Lebovits A.** Permeability of polymers to gases, vapors, and liquids. *Modern Plastics* 43: 139–150, 196–213, 1966.
22. **Lerman J, Gregory GA, Willis MM, and Eger EI II.** Age and solubility of volatile anesthetics in blood. *Anesthesiology* 61: 139–143, 1984.
23. **Mastenbrook SM Jr, Dempsey JA, and Massaro TA.** Ventilation-perfusion ratio distributions by mass spectrometry with membrane catheters. *J Appl Physiol* 53: 770–778, 1982.
24. **Mastenbrook SM Jr, Massaro TA, and Dempsey JA.** Multiple gas measurements at trace levels with a quadrupole mass spectrometer: gas phase calibration. *J Appl Physiol* 44: 634–639, 1978.
25. **Michaels AS and Bixler HJ.** Membrane permeation: theory and practice. In: *Progress in Separation and Purification*, edited by E. Perry. New York: Interscience, 1968, p. 143–186.
26. **Moinard J, Manier G, Pillet O, and Castaing Y.** Effect of inhaled nitric oxide on hemodynamics and $\dot{V}A/\dot{Q}$ inequalities in patients with chronic obstructive pulmonary disease. *Am J Respir Crit Care Med* 149: 1482–1487, 1994.
27. **Prediletto R, Formichi B, Begliomini E, Fornai E, Viegi G, Ruschi S, Paoletti P, Giannella AN, Santolicandro A, and Giuntini C.** Ventilation-perfusion heterogeneity and gas exchange variables in acute pulmonary embolism evaluated by two different computerized techniques. *Int J Clin Monit Comput* 5: 221–227, 1988.
28. **Putensen C, Rasanen J, Lopez FA, and Downs JB.** Effect of interfacing between spontaneous breathing and mechanical cycles on the ventilation-perfusion distribution in canine lung injury. *Anesthesiology* 81: 921–930, 1994.
29. **Roca J, Ramis LI, Rodriguez-Roisin R, Ballester E, Montserrat JM, and Wagner PD.** Serial relationships between ventilation-perfusion inequality and spirometry in acute severe asthma requiring hospitalization. *Am Rev Respir Dis* 137: 1055–1061, 1988.
30. **Shimazu T, Yukioka T, Ikeuchi H, Mason AD Jr, Wagner PD, and Pruitt BA Jr.** Ventilation-perfusion alterations after smoke inhalation injury in an ovine model. *J Appl Physiol* 81: 2250–2259, 1996.
31. **Snedden W, LeDez K, and Manson HJ.** A new method for the measurement of gas solubility. *J Appl Physiol* 80: 1371–1378, 1996.
32. **Souders JE, George SC, Polissar NL, Swenson ER, and Hlastala MP.** Tracheal gas exchange: perfusion-related differences in inert-gas elimination. *J Appl Physiol* 79: 918–928, 1995.
33. **Tenling A, Hachenberg T, Tyden H, Wegenius G, and Hedenstierna G.** Atelectasis and gas exchange after cardiac surgery. *Anesthesiology* 89: 371–378, 1998.
34. **Tokics L, Hedenstierna G, Svensson L, Brismar B, Cederlund T, Lundquist H, and Strandberg A.** $\dot{V}A/\dot{Q}$ distribution and correlation to atelectasis in anesthetized paralyzed humans. *J Appl Physiol* 81: 1822–1833, 1996.
35. **Wagner PD, Laravuso RB, Goldzimmer E, Naumann PF, and West JB.** Distributions of ventilation-perfusion ratios in dogs with normal and abnormal lungs. *J Appl Physiol* 38: 1099–1109, 1975.
36. **Wagner PD, Laravuso RB, Uhl RR, and West JB.** Continuous distributions of ventilation-perfusion ratios in normal subjects breathing air and 100% O_2. *J Clin Invest* 54: 54–68, 1974.
37. **Wagner PD and Lopez FA.** Gas chromatography techniques in respiratory physiology. In: *Techniques in the Life Sciences*, edited by Otis AB. County Clare, Ireland: Elsevier, 1984, p. 1–24.
38. **Wagner PD, Naumann PF, and Laravuso RB.** Simultaneous measurement of eight foreign gases in blood by gas chromatography. *J Appl Physiol* 36: 600–605, 1974.
39. **Wagner PD and Rodriguez-Roisin R.** Clinical advances in pulmonary gas exchange. *Am Rev Respir Dis* 143: 883–888, 1991.
40. **Wagner PD, Saltzman HA, and West JB.** Measurement of continuous distributions of ventilation-perfusion ratios: theory. *J Appl Physiol* 36: 588–599, 1974.
41. **Westover LB, Tou JC, and Mark JH.** Novel mass spectrometric sampling device–hollow fiber probe. *Anal Chem* 46: 568–571, 1974.
42. **Woldring S.** Tutorial: biomedical application of mass spectrometry for monitoring pressures. A technical review. *J Assoc Advan Med Instr* 4: 43–56, 1970.
43. **Yamaguchi K, Mori M, Kawai A, Takasugi T, Asano K, Oyamada Y, Aoki T, Fujita H, Suzuki Y, Yamasawa F, and Kawashiro T.** Ventilation-perfusion inequality and diffusion impairment in acutely injured lungs. *Respir Physiol* 98: 165–177, 1994.
44. **Zavala E, Ferrer M, Polese G, Masclans JR, Planas M, Milic-Emili J, Rodriguez-Roisin R, Roca J, and Rossi A.** Effect of inverse I:E ratio ventilation on pulmonary gas exchange in acute respiratory distress syndrome. *Anesthesiology* 88: 35–42, 1998.